

# ALIGN-RUDDER: LEARNING FROM FEW DEMONSTRATIONS BY REWARD REDISTRIBUTION

Vihang P. Patil\* Markus Hofmarcher\* Marius-Constantin Dinu\* Matthias Dorfer<sup>‡</sup>  
 Patrick M. Blies<sup>‡</sup> Johannes Brandstetter\* Jose A. Arjona-Medina\* Sepp Hochreiter\*,<sup>†</sup>

\*ELLIS Unit Linz and LIT AI Lab,  
 Institute for Machine Learning,  
 Johannes Kepler University Linz, Austria

<sup>†</sup>Institute of Advanced Research in Artificial Intelligence (IARAI)

<sup>‡</sup>enliteAI, Vienna, Austria

## ABSTRACT

Reinforcement Learning algorithms require a large number of samples to solve complex tasks with sparse and delayed rewards. Complex tasks can often be hierarchically decomposed into sub-tasks. A step in the  $Q$ -function can be associated with solving a sub-task, where the expectation of the return increases. RUDDER has been introduced to identify these steps and then redistribute reward to them, thus immediately giving reward if sub-tasks are solved. Since the problem of delayed rewards is mitigated, learning is considerably sped up. However, for complex tasks, current exploration strategies as deployed in RUDDER struggle with discovering episodes with high rewards. Therefore, we assume that episodes with high rewards are given as demonstrations and do not have to be discovered by exploration. Typically the number of demonstrations is small and RUDDER’s LSTM model as a deep learning method does not learn well. Hence, we introduce Align-RUDDER, which is RUDDER with two major modifications. First, Align-RUDDER assumes that episodes with high rewards are given as demonstrations, replacing RUDDER’s safe exploration and lessons replay buffer. Second, we replace RUDDER’s LSTM model by a profile model that is obtained from multiple sequence alignment of demonstrations. Profile models can be constructed from as few as two demonstrations as known from bioinformatics. Align-RUDDER inherits the concept of reward redistribution, which considerably reduces the delay of rewards, thus speeding up learning. Align-RUDDER outperforms competitors on complex artificial tasks with delayed reward and few demonstrations. On the MineCraft ObtainDiamond task, Align-RUDDER is able to mine a diamond, though not frequently.

## INTRODUCTION

**Overview over our new method, Align-RUDDER<sup>1</sup>.** Reinforcement learning algorithms struggle with learning complex tasks that have sparse and delayed rewards (Sutton & Barto, 2018; Rahmandad et al., 2009; Luoma et al., 2017). RUDDER (Arjona-Medina et al., 2019) has been shown to excel for learning sparse and delayed rewards. RUDDER requires episodes with high rewards, to store them in its lessons replay buffer for learning. However, for complex tasks episodes with high rewards are difficult to find by current exploration strategies. Humans and animals obtain high reward episodes by teachers, role models, or prototypes. In this context, we assume that episodes with high rewards are given as demonstrations. Consequently, RUDDER’s safe exploration and lessons replay buffer can be replaced by these demonstrations. Generating demonstrations is often tedious for humans and time-consuming for automated exploration strategies, therefore typically only few demonstrations are available. However, RUDDER’s LSTM as a deep learning method requires many examples for learning. Therefore, we replace RUDDER’s LSTM by a profile model obtained from multiple sequence alignment of the demonstrations. Profile models are well known in bioinformatics, where

<sup>1</sup>Code available at: <https://github.com/ml-jku/align-rudder>

they are used to score new sequences according to their sequence similarity to the aligned sequences. RUDDER’s LSTM predicts the return for an episode given an action-state sub-sequence. In our new method, Align-RUDDER, the LSTM prediction is replaced by the score of this sub-sequence if aligned to the profile model. In the RUDDER implementation, the LSTM predictions are used for return decomposition and reward redistribution by using the difference of consecutive predictions. Align-Rudder performs return decomposition and reward redistribution via the difference of alignment scores for consecutive sub-sequences.

**Align-RUDDER vs. temporal difference and Monte Carlo.** We assume to have high reward episodes as demonstrations. Align-RUDDER uses these episodes to identify state-actions that are indicative for high rewards through alignment techniques. Next, Align-RUDDER redistributes rewards to these state-actions, which enable to adjust a policy so that these state-actions are reached more often. Consequently, the return is increased and relevant episodes are sampled more frequently. For *delayed rewards* and *model-free* reinforcement learning: (I) temporal difference (TD) suffers from vanishing information even with eligibility traces (Arjona-Medina et al., 2019); (II) Monte Carlo (MC) has to average over all possible futures, which leads to high variance (Arjona-Medina et al., 2019). If models are available as they are for GO and chess, model-based methods like Monte-Carlo Tree Search (MCTS) can handle delayed and rare rewards (Silver et al., 2016; 2017).

**Basic insight: Q-functions (action-value functions) are step functions.** Complex tasks are characterized by a hierarchical structure consisting of sub-tasks or sub-goals (see first row in left panel of Fig. 1). The  $Q$ -function of an optimal policy resembles a step function. A step in the  $Q$ -function is a change in return expectation, that is, the expected amount of the return or the probability to obtain the return changes. Steps indicate achievements, failures, accomplishing sub-tasks, achieving a sub-goal, or changes of the environment. To identify large steps is important for speeding up learning considerably: knowing the large steps in the  $Q$ -function allows (i) to increase the return and (ii) to sample more relevant episodes.

A  $Q$ -function must predict the expected return from every state-action pair. Therefore, it is prone to make a prediction error at some point, which might hamper learning (see second row in left panel of Fig. 1). Since the  $Q$ -function is mostly constant, it is not necessary to predict the expected return for every state-action pair. It is sufficient to *identify relevant state-actions* across the whole episode and use them for predicting the expected return (see third row in left panel of Fig. 1). The LSTM network (Hochreiter & Schmidhuber, 1995; 1997a;b) is perfectly suited to store only the relevant state-actions in its memory cells. It only updates them if a new relevant state-action pair appears, consequently its output is constant until the memory cells are updated. The basic insight that  $Q$ -functions are step functions is the motivation for identifying these steps via return decomposition and speeding up learning via reward redistribution.

**Reward Redistribution: Idea and return decomposition.** We consider reward redistributions that are obtained by return decomposition given an episodic Markov decision process (MDP). The  $Q$ -function is assumed to be a step function (blue curve in first row in right panel of Fig. 1). Return decomposition identifies the steps of the  $Q$ -function (green arrows in right panel Fig. 1). A function predicts (LSTM in RUDDER, alignment model in Align-RUDDER) the expected return (big red arrow in first row in right panel of Fig. 1) given the state-action sub-sequence. The prediction is decomposed into single steps of the  $Q$ -function (green arrows in Fig. 1). The redistributed rewards (small red arrows in second and third row of right panel of Fig. 1) remove the steps. Consequently, the expected future reward is equal to zero (blue curve at zero in last row in right panel of Fig. 1). Having future rewards of zero means that learning the  $Q$ -values simplifies to estimating the expected immediate rewards (small red arrows in right panel of Fig. 1), since delayed rewards are no longer present.

**Reward redistribution using multiple sequence alignment.** RUDDER uses an LSTM model for reward redistribution via return decomposition. The reward redistribution is the difference of two subsequent predictions of the LSTM model. If a state-action pair increases the prediction of the return, then it is immediately rewarded. Using state-action sub-sequences  $(s, a)_{0:t} = (s_0, a_0, \dots, s_t, a_t)$ , the redistributed reward is  $R_{t+1} = g((s, a)_{0:t}) - g((s, a)_{0:t-1})$ , where  $g$  is an LSTM model that predicts the return of the episode. The LSTM model first learns to approximate the largest steps of the  $Q$ -function, since they reduce the prediction error the most. Therefore the LSTM model extracts first the relevant state-actions pairs (events).

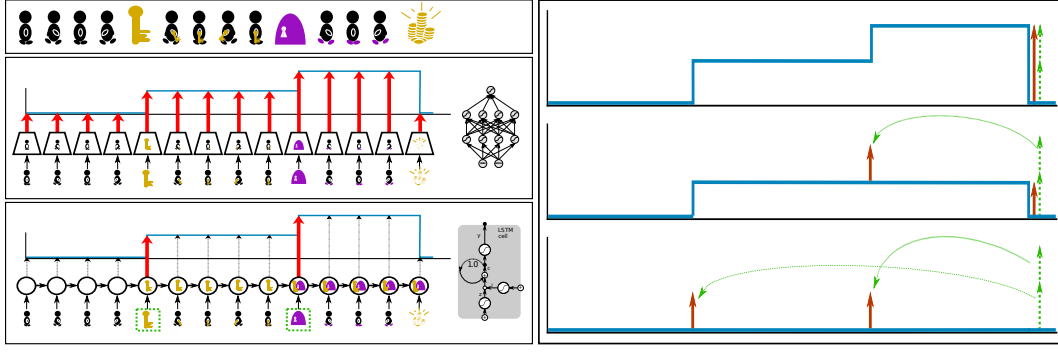


Figure 1: **Basic insight of RUDDER (left panel) and reward redistribution (right panel).** **Left panel first row:** An agent has to take a key to open the door to a treasure. Both events increase the probability of obtaining the treasure. **Left panel second row:** Learning the  $Q$ -function by a fully connected network requires to predict the expected return from every state-action pair (red arrows). **Left panel third row:** Learning the  $Q$ -functions by memorizing relevant state-action pairs requires only to predict the steps (red arrows). **Right panel first row:** The  $Q$ -function is the future expected reward (blue curve) since reward is given only at the end. The  $Q$ -function is a step function, where green arrows indicate steps and the big red arrow the expected return. **Right panel second row:** The redistributed reward (small red arrow) removes a step in the  $Q$ -function and the future expected return becomes constant at this step (blue curve). **Right panel third row:** After redistributing the whole return, the expected future reward is equal to zero everywhere (blue curve at zero). Learning has only to estimate the expected immediate reward (red arrows) since delayed rewards are no longer present.

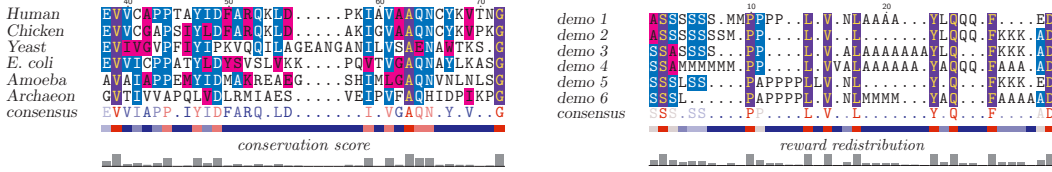


Figure 2: Left panel: Alignment of biological sequences (triosephosphate isomerase) giving a conservation score. Right panel: Alignment of demonstrations using the conservation score for reward redistribution.

We now use techniques from sequence alignment to replace the LSTM model by a profile model. The profile model is the result of a multiple sequence alignment of the demonstrations and allows aligning new sequences to it. Both the sub-sequences  $(s, a)_{0:t-1}$  and  $(s, a)_{0:t}$  are mapped to sequences of events and then are aligned to the profile model. Thus, both sequences receive a score  $S$ , which is proportional to the function  $g$ . The redistributed reward is again  $R_{t+1} = g((s, a)_{0:t}) - g((s, a)_{0:t-1})$  (see Eq. (5)). Figure 2 shows at the left panel an alignment of biological sequences and at the right panel an alignment of demonstrations. The concepts of reward redistribution and return decomposition are reviewed in Sec. and reward redistribution by sequence alignment is explained in Sec. .

**Related work.** Learning from demonstrations has been widely studied over the last 50 years (Billard et al., 2008). The most prominent example is imitation learning, which profits from supervised techniques when the number of available demonstrations is large enough (Michie et al., 1990; Pomerleau, 1991; Michie & Camacho, 1994; Schaal, 1996; Kakade & Langford, 2002). However, policies trained with imitation learning tend to drift away from demonstration trajectories due to a distribution shift (Ross & Bagnell, 2010), which effect can be mitigated (III et al., 2009; Ross & Bagnell, 2010; Ross et al., 2011; Judah et al., 2014; Sun et al., 2017; 2018). Many approach use the demonstrations for initialization, e.g. of policy networks (Taylor et al., 2011; Silver et al., 2016; Rajeswaran et al., 2018; Le et al., 2018), value function networks (Hester et al., 2017; 2018), both networks (Zhang & Ma, 2018; Nair et al., 2018), or an experience replay buffer (Hosu & Rebedea, 2016; Vecerík et al., 2017). Beyond initialization, demonstrations are used to define constraints (Kim et al., 2013), generate sub-goals (Eysenbach et al., 2019), enforce regularization (Reddy et al., 2020), guide exploration (Subramanian et al., 2016; Jing et al., 2019), or shape rewards (Judah et al.,

2014; Brys et al., 2015; Suay et al., 2016). Demonstrations may serve for inverse reinforcement learning (Ng & Russell, 2000; Abbeel & Ng, 2004; Ho & Ermon, 2016), which aims at learning a (non-sparse) reward function that best explains the demonstrations. Again learning reward functions requires a large number of demonstrations (Syed & Schapire, 2007; Ziebart et al., 2008; Tucker et al., 2018; Silva et al., 2019). Some approaches rely on few-shot or/and meta learning, but a large set of auxiliary tasks is required (Duan et al., 2017; Finn et al., 2017; Zhou et al., 2020). Concluding, most methods that learn from demonstrations rely on the availability of many demonstrations (Kharon, 1999; Lopes et al., 2009), in particular, if using deep learning methods (Bengio & Lecun, 2007; Lakshminarayanan et al., 2016). Some methods can learn on few demonstrations like Imitation Learning via Regularized Behavioral Cloning (SQIL) (Reddy et al., 2020), Generative Adversarial Imitation Learning (GAIL) (Ho & Ermon, 2016), and Deep  $Q$ -learning from Demonstrations (DQfD) (Hester et al., 2018).

## REVIEW REWARD REDISTRIBUTION

Reward redistribution and return decomposition are concepts introduced in RUDDER (Arjona-Medina et al., 2019) and are the fundamental concepts of our Align-RUDDER, too. Reward redistribution based on return decomposition eliminates – or at least mitigates – delays of rewards while preserving the same optimal policies. Align-RUDDER is justified by the theory of return decomposition and reward redistribution when using multiple sequence alignment for constructing a reward redistribution model. In this section, we briefly review the concepts and theory of return decomposition and reward redistribution.

**Preliminaries.** We consider a finite MDP defined by the 5-tuple  $\mathcal{P} = (\mathcal{S}, \mathcal{A}, \mathcal{R}, p, \gamma)$  where the state space  $\mathcal{S}$  and the action space  $\mathcal{A}$  are sets of finite states  $s$  and actions  $a$  and  $\mathcal{R}$  the set of bounded rewards  $r$ . For a given time step  $t$ , the corresponding random variables are  $S_t$ ,  $A_t$  and  $R_{t+1}$ . Furthermore,  $\mathcal{P}$  has transition-reward distributions  $p(S_{t+1} = s', R_{t+1} = r \mid S_t = s, A_t = a)$ , and a discount factor  $\gamma \in (0, 1]$ , which we keep at  $\gamma = 1$ . A Markov policy  $\pi(a \mid s)$  is a probability of an action  $a$  given a state  $s$ . We consider finite time horizon MDPs or MDPs with an absorbing state. The discounted return of a sequence of length  $T$  at time  $t$  is  $G_t = \sum_{k=0}^{T-t} \gamma^k R_{t+k+1}$ . As usual, the  $Q$ -function for a given policy  $\pi$  is  $q^\pi(s, a) = \mathbb{E}_\pi[G_t \mid S_t = s, A_t = a]$ .  $\mathbb{E}_\pi[x \mid s, a]$  is the expectation of  $x$ , where the random variable is a sequence of states, actions, and rewards that is generated with transition-reward distribution  $p$ , policy  $\pi$ , and starting at  $(s, a)$ . The goal is to find an optimal policy  $\pi^* = \operatorname{argmax}_\pi \mathbb{E}_\pi[G_0]$  maximizing the expected return at  $t = 0$ . We assume that the states  $s$  are time-aware (time  $t$  can be extracted from each state) in order to assure stationary optimal policies. According to Proposition 4.4.3 in (Puterman, 2005), a deterministic optimal policy  $\pi^*$  exists.

**Definitions.** A *sequence-Markov decision process* (SDP) is defined as a decision process that has Markov transition probabilities but a reward probability that is not required to be Markov. Two SDPs  $\tilde{\mathcal{P}}$  and  $\mathcal{P}$  with different reward probabilities are *return-equivalent* if they have the same expected return at  $t = 0$  for each policy  $\pi$ , and *strictly return-equivalent* if they additionally have the same expected return for every episode. Since for every  $\pi$  the expected return at  $t = 0$  is the same, return-equivalent SDPs have the same optimal policies. A *reward redistribution* is a procedure that—for a given sequence of a delayed reward SDP  $\tilde{\mathcal{P}}$ —redistributes the realization or expectation of its return  $\tilde{G}_0$  along the sequence. This yields a new SDP  $\mathcal{P}$  with  $R$  as random variable for the redistributed reward and the same optimal policies as  $\tilde{\mathcal{P}}$ :

**Theorem 1** (Arjona-Medina et al. (2019)). *Both the SDP  $\tilde{\mathcal{P}}$  with delayed reward  $\tilde{R}_{t+1}$  and the SDP  $\mathcal{P}$  with redistributed reward  $R_{t+1}$  have the same optimal policies.*

The delay of rewards is captured by the *expected future rewards*  $\kappa(m, t - 1)$  at time  $(t - 1)$ .  $\kappa$  is defined as  $\kappa(m, t - 1) := \mathbb{E}_\pi[\sum_{\tau=0}^m R_{t+1+\tau} \mid s_{t-1}, a_{t-1}]$ , that is, at time  $(t - 1)$  the expected sum of future rewards from  $R_{t+1}$  to  $R_{t+1+m}$  but not the immediate reward  $R_t$ . A reward redistribution is defined to be *optimal*, if  $\kappa(T - t - 1, t) = 0$  for  $0 \leq t \leq T - 1$ , which is equivalent to  $\mathbb{E}[R_{t+1} \mid s_{t-1}, a_{t-1}, s_t, a_t] = \tilde{q}^\pi(s_t, a_t) - \tilde{q}^\pi(s_{t-1}, a_{t-1})$ :

**Theorem 2** (Arjona-Medina et al. (2019)). *We assume a delayed reward MDP  $\tilde{\mathcal{P}}$ , with episodic reward. A new SDP  $\mathcal{P}$  is obtained by a second order Markov reward redistribution, which ensures*

that  $\mathcal{P}$  is return-equivalent to  $\tilde{\mathcal{P}}$ . For a specific  $\pi$ , the following two statements are equivalent:

(I)  $\kappa(T - t - 1, t) = 0$ , i.e. the reward redistribution is optimal,

(II)  $E[R_{t+1} | s_{t-1}, a_{t-1}, s_t, a_t] = \tilde{q}^\pi(s_t, a_t) - \tilde{q}^\pi(s_{t-1}, a_{t-1})$ . (1)

An optimal reward redistribution fulfills for  $1 \leq t \leq T$  and  $0 \leq m \leq T - t$ :  $\kappa(m, t - 1) = 0$ .

This theorem shows that an optimal reward redistribution relies on steps  $\tilde{q}^\pi(s_t, a_t) - \tilde{q}^\pi(s_{t-1}, a_{t-1})$  of the  $Q$ -function. Identifying the largest steps in the  $Q$ -function detects the largest rewards that have to be redistributed, which makes the largest progress towards obtaining an optimal reward redistribution. If the reward redistribution is optimal, the  $Q$ -values of  $\mathcal{P}$  are given by  $q^\pi(s_t, a_t) = \tilde{q}^\pi(s_t, a_t) - \psi^\pi(s_t)$  and therefore  $\tilde{\mathcal{P}}$  and  $\mathcal{P}$  have the same advantage function:

**Theorem 3** (Arjona-Medina et al. (2019)). *If the reward redistribution is optimal, then the  $Q$ -values of the SDP  $\mathcal{P}$  are*

$$q^\pi(s_t, a_t) = r(s_t, a_t) = \tilde{q}^\pi(s_t, a_t) - E_{s_{t-1}, a_{t-1}}[\tilde{q}^\pi(s_{t-1}, a_{t-1}) | s_t] = \tilde{q}^\pi(s_t, a_t) - \psi^\pi(s_t). \quad (2)$$

The SDP  $\mathcal{P}$  and the original MDP  $\tilde{\mathcal{P}}$  have the same advantage function.

For an optimal reward redistribution only the expectation of the immediate reward  $r(s_t, a_t) = E[R_{t+1} | s_t, a_t]$  must be estimated. This considerably simplifies learning.

**Learning methods according to Arjona-Medina et al. (2019).** The  $Q$ -values can be estimated directly according to Eq. (2) assuming an optimal redistribution (Type A variant i).  $Q$ -values can be corrected for a non-optimal reward redistribution by additionally estimating  $\kappa$  (Type A variant ii).  $Q$ -value estimation can use eligibility traces (Type A variant iii). The redistributed rewards can be used for policy gradients (Type B) or for TD learning ( $Q$ -learning) if immediate and future reward are drawn together (Type C). For all these learning methods, demonstrations can be used for initialization (e.g. experience replay buffer) or pre-training (e.g. policy network with behavioral cloning).

**Non-optimal reward redistribution and Align-RUDDER.** According to Theorem 1, non-optimal reward redistributions do not change the optimal policies. The value  $\kappa(T - t - 1, t)$  measures the remaining delayed reward. The smaller  $\kappa$  is, the faster is the learning process. For Monte Carlo (MC) estimates, smaller  $\kappa$  reduces the variance of the future rewards, and, therefore the variance of the estimation. For temporal difference (TD) estimates, smaller  $\kappa$  reduces the amount of information that has to flow back. Align-RUDDER dramatically reduces the amount of delayed rewards by identifying key events via multiple sequence alignment, to which reward is redistributed. For an episodic MDP, a reward that is redistributed to time  $t$  reduces all  $\kappa(m, \tau)$  with  $t \leq \tau < T$  by the expectation of the reward. Therefore, in most cases Align-RUDDER makes  $\kappa$ -values much smaller.

## REWARD REDISTRIBUTION BY SEQUENCE ALIGNMENT

In bioinformatics, sequence alignment identifies similarities between biological sequences to determine their evolutionary relationship (Needleman & Wunsch, 1970; Smith & Waterman, 1981). Align-RUDDER uses such alignment techniques to align two or more demonstrations with high return. We assume that the demonstrations follow the same underlying strategy, therefore they are similar to each other and can be aligned. The alignment provides a profile model given as a consensus sequence (the strategy), a frequency matrix, or a Position-Specific Scoring Matrix (PSSM) (Stormo et al., 1982). The redistributed reward of a new sequence is the difference of the scores of consecutive sub-sequences when aligned to the profile model. The new reward redistribution approach consists of five steps as depicted in Figure 3: (I) Define events to turn episodes of state-action sequences into sequences of events. (II) Determine an alignment scoring scheme according to Eq. (3), so that relevant events are aligned to each other. (III) Perform a multiple sequence alignment of the demonstrations. (IV) (a) Compute the profile model and (b) the PSSM according to Eq. (4). (V) Redistribute the reward: Each sub-sequence  $\tau_t$  of a new episode  $\tau$  is aligned to the profile. The redistributed reward  $R_{t+1}$  is proportional to the difference of scores  $S$  based on the PSSM given in Eq. (4), i.e.  $R_{t+1} \propto S(\tau_t) - S(\tau_{t-1})$ .

**(I) Defining Events.** Alignment techniques assume sequences that consist of few symbols, e.g. about 20 symbols. An alignment is only reliable if many equal (or similar) symbols are aligned. Therefore, episodes must be described as sequences of events, where the number of events should be small. These events can be the original state-action pairs, clusters thereof, or other representations of



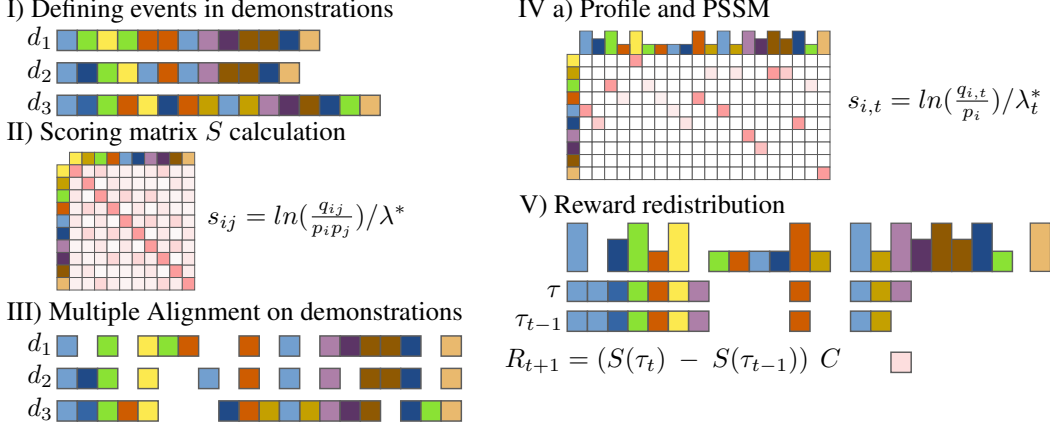


Figure 3: The five steps of Align-RUDDER’s reward redistribution.

state-action pairs. Examples are possession of items, inventory, received reward, health, energy, or skill level status, and similar. It should be possible to describe the strategy by these events.

In general, we define events as a cluster of states or state-actions. A sequence of events is obtained from a state-action sequence by substituting states or state-actions by their cluster identifier. In order to cluster states, a similarity measure between them is required. We suggest to use the “successor representation” (Dayan, 1993) of the states, which gives a similarity matrix based on how connected two states are given a policy. Successor representation have been used before (Machado et al., 2017; Ramesh et al., 2019) to obtain important events, for option learning. For computing the successor representation, we use the demonstrations combined with state-action sequences generated by a random policy. For high dimensional state spaces “successor features” (Barreto et al., 2017) can be used. We use similarity-based clustering methods like affinity propagation (AP) (Frey & Dueck, 2007). For AP the similarity matrix does not have to be symmetric and the number of clusters need not be known. State action pairs  $(s, a)$  are mapped to events  $e$  by a function  $f$ :  $e = f(s, a)$ .

**(II) Determining the Alignment Scoring System.** Alignment algorithms require a scoring system that allows to distinguish similar sequences from dissimilar sequences. A scoring matrix  $\$$  has entries  $\$_{i,j}$  that give the score for aligning event  $i$  with  $j$ . The total score  $S$  of a multiple sequence alignment is the sum of all pairwise scores:  $S = \sum_{i,j,i < j} \sum_{t=0}^L \$_{x_{i,t}, x_{j,t}}$ , where  $x_{i,t}$  means that event  $x_{i,t}$  is at position  $t$  for sequence  $\tau_i = e_{i,0:T}$  in the alignment, analog for  $x_{j,t}$  and the sequence  $\tau_j = e_{j,0:T}$ , and  $L$  is the alignment length. Note that  $L \geq T$  and  $x_{i,t} \neq e_{i,t}$ , since gaps are present in the alignment.

In the alignment, events should have the same probability of being aligned as they would have if we know the strategy and align demonstrations accordingly. The theory of high scoring segments allows us to derive such a scoring scheme (Karlin & Altschul, 1990; Karlin et al., 1990; Altschul et al., 1990). Event  $i$  is observed with probability  $p_i$  in the demonstrations, therefore a random alignment aligns event  $i$  with  $j$  with probability  $p_i p_j$ . An alignment algorithm maximizes the total score  $S$  and, thereby, aligns events  $i$  and  $j$  with probability  $q_{ij}$ . High values of  $q_{ij}$  means that the algorithm often aligns events  $i$  and  $j$  using the scoring matrix  $\$$  with entries  $\$_{i,j}$ . According to Theorem 2 and Equation [3] in (Karlin & Altschul, 1990), asymptotically with the sequence length, we have

$$\$_{i,j} = \ln(q_{ij} / (p_i p_j)) / \lambda^*, \quad (3)$$

where  $\lambda^*$  is the single unique positive root of  $\sum_{i=1}^n \sum_{j=1}^n p_i p_j \exp(\lambda \$_{i,j}) = 1$  (Equation [4] in Karlin & Altschul (1990)).

We can now choose a desired probability  $q_{ij}$  and then compute the scoring matrix  $\$$  with entries  $\$_{i,j}$ . High values of  $q_{ij}$  should indicate relevant events for the strategy. A priori, we only know that a relevant event should be aligned to itself, while we do not know which events are relevant. Therefore we set  $q_{ij}$  to large values for every  $i = j$  and to low values for  $i \neq j$ . Concretely, we set  $q_{ij} = p_i - \epsilon$  for  $i = j$  and  $q_{ij} = \epsilon / (n - 1)$  for  $i \neq j$ , where  $n$  is the number of different possible events. Events with smaller  $p_i$  receive a higher score  $\$_{i,i}$  when aligned to themselves since this self-match is less

often observed when randomly matching events ( $p_i p_i$  is the probability of a random self-match). Any prior knowledge about events should be incorporated into  $q_{ij}$ .

**(III) Multiple sequence alignment (MSA).** MSA first produces pairwise alignments between all demonstrations. Afterwards, a guiding tree is produced via hierarchical clustering, which clusters the sequences according to their pairwise alignment scores. Demonstrations which follow the same strategy appear in the same cluster in the guiding tree. Each cluster is aligned separately via MSA to address different strategies. MSA methods like ClustalW (Thompson et al., 1994) or MUSCLE (Edgar, 2004) can be used.

**(IV) Position-Specific Scoring Matrix (PSSM) and Profile.** From the final alignment, we construct a) an MSA profile (column-wise event frequencies  $q_{i,j}$ ) and b) a PSSM (Stormo et al., 1982) which is used for aligning new sequences to the profile of the MSA. To compute the PSSM (column-wise scores  $s_{i,t}$ ), we apply Theorem 2 and Equation [3] in (Karlin & Altschul, 1990). Event  $i$  is observed with probability  $p_i$  in the data. For each position  $t$  in the alignment, we compute  $q_{i,t}$ , which indicates the frequency of event  $i$  at position  $t$ . The PSSM is

$$s_{i,t} = \ln(q_{i,t}/p_i)/\lambda_t^*, \quad (4)$$

where  $\lambda_t^*$  is the single unique positive root of  $\sum_{i=1}^n p_i \exp(\lambda s_{i,t}) = 1$  (Equation [1] in Karlin & Altschul (1990)). Again, if we align a new sequence that follows the underlying strategy (a new demonstration) to the profile model, then we would see that event  $i$  is aligned to position  $t$  in the profile with probability  $q_{i,t}$ .

**(V) Reward Redistribution.** Our reward redistribution is based on the profile model. A sequence  $\tau = e_{0:T}$  ( $e_t$  is event at position  $t$ ) can be aligned to the profile, giving the score  $S(\tau) = \sum_{t=0}^L s_{x_t,t}$ , where  $s_{i,t}$  is the alignment score for event  $i$  at position  $t$ ,  $x_t$  is the event at position  $t$  of sequence  $\tau$  in the alignment, and  $L$  is the profile length. Note that  $L \geq T$  and  $x_t \neq e_t$ , since gaps are present in the alignment. If  $\tau_t = e_{0:t}$  is the prefix sequence of  $\tau$  of length  $t + 1$ , then the reward redistribution is

$$R_{t+1} = (S(\tau_t) - S(\tau_{t-1})) C = g((s, a)_{0:t}) - g((s, a)_{0:t-1}), \quad (5)$$

$$R_{T+2} = \tilde{G}_0 - \sum_{t=0}^T R_{t+1}, \quad C = \frac{\mathbb{E}_{\text{demo}} [\tilde{G}_0]}{\mathbb{E}_{\text{demo}} [\sum_{t=0}^T S(\tau_t) - S(\tau_{t-1})]},$$

where  $\tilde{G}_0 = \sum_{t=0}^T \tilde{R}_{t+1}$  is the original return of the sequence  $\tau$  and  $S(\tau_{-1}) = 0$ .  $\mathbb{E}_{\text{demo}}$  is the expectation over demonstrations, and  $C$  scales  $R_{t+1}$  to the range of  $\tilde{G}_0$ .  $R_{T+2}$  is the correction of the redistributed reward (Arjona-Medina et al., 2019), with zero expectation for demonstrations:  $\mathbb{E}_{\text{demo}} [R_{T+2}] = 0$ . Since  $\tau_t = e_{0:t}$  and  $e_t = f(s_t, a_t)$ , we can set  $g((s, a)_{0:t}) = S(\tau_t)C$ . We ensure strict return equivalence, since  $G_0 = \sum_{t=0}^{T+1} R_{t+1} = \tilde{G}_0$ . The redistributed reward depends only on the past, that is,  $R_{t+1} = h((s, a)_{0:t})$ . For computational efficiency, the profile alignment of  $\tau_{t-1}$  can be extended to a profile alignment for  $\tau_t$  like exact matches are extended to high-scoring sequence pairs with the BLAST algorithm (Altschul et al., 1990; 1997).

## EXPERIMENTS

Align-RUDDER is compared on two artificial tasks with sparse & delayed rewards and few demonstrations to Behavioral Cloning with  $Q$ -learning (BC+ $Q$ ) and Deep  $Q$ -learning from Demonstrations (DQfD) (Hester et al., 2018). GAIL (Ho & Ermon, 2016), which has been designed for control in continuous observation spaces, failed to solve the two artificial tasks, as reported previously for similar tasks (Reddy et al., 2020). Then, we test Align-RUDDER on the complex MineCraft ObtainDiamond task with episodic, therefore highly delayed, rewards (Guss et al., 2019b). All experiments use finite time horizon MDPs with  $\gamma = 1$  and episodic reward. More details in appendix Section A.3.

**Artificial tasks (I) and (II).** They are variations of the gridworld *rooms example* (Sutton et al., 1999), where cells (locations) are the states of the MDP. In our setting the states do not have to be time-aware for ensuring an MDP but the unobserved used-up time introduces a random effect. The grid is divided into different rooms which are only connected by a single cell. The goal of the agent is to reach a target from an initial state with the fewest steps possible. It has to cross different rooms,

which are connected by doors, except for the first room, which is only connected to the second room by a *portal*. If the agent is at the portal entry cell of the first room then it is teleported to a fixed portal arrival cell in the second room. The location of the portal entry cell is randomly chosen for every episode, while the portal arrival cell is fixed across episodes. The location of portal entry cell is given in the state for the first room. The portal is introduced to avoid that BC initialization alone solves the task. It enforces that going to the portal entry cells is learned, when they are at positions not observed in demonstrations. At every location, the agent can move *up*, *down*, *left*, *right* if it stays on the grid. The state transitions are stochastic, except for teleportation. An episode ends after  $T = 200$  time steps. If the agent arrives at the target location, then at the next step it goes into an absorbing state where it stays until  $T = 200$  without receiving further rewards. Reward is only given at the end of the episode. The final reward is 3 when reaching the target, and 1 otherwise. To enforce that the agent reaches the goal with the fewest steps possible, a small negative reward of  $-0.01$  is given at every time step. Demonstrations are generated by an optimal policy with an exploration rate of 0.2.

Next we describe the five steps of Align-RUDDER’s reward redistribution: (1) Events correspond to clusters of states obtained by Affinity Propagation (Frey & Dueck, 2007) using as similarity the successor representation of the states based on demonstrations. (2) The scoring matrix is obtained by Eq. (3) using  $\epsilon = 0$  and setting all off-diagonal values of the scoring matrix to  $-1$ . (3) ClustalW is used for the MSA of the demonstrations with all gap penalties set to zero and without using biological options. (4) The MSA supplies a profile model and a PSSM as in Eq. (4). (5) Sequences that are generated by the agent are mapped to sequences of events according to step (1). Reward is redistributed via differences of profile alignment scores of consecutive sub-sequences according to Eq. (5) using the PSSM from step (4).

**Sub-tasks.** The reward redistribution implicitly defines sub-tasks, which are alignment positions with receive high redistributed reward (doors and portal arrival). The sub-tasks partition the  $Q$ -table into sub-tables that represent a sub-agent. In the tabular case, defining sub-tasks has not effect on learning if compared to a single  $Q$ -table.

All compared methods learn a  $Q$ -table and use an  $\epsilon$ -greedy policy with  $\epsilon = 0.2$ . The  $Q$ -table is initialized by behavioral cloning (BC). The state-action pairs which are not initialized since they are not visited in the demonstrations get an optimistic initialization by drawing a sample from a normal distribution estimated from demonstration returns (avoiding equal  $Q$ -values). Align-RUDDER learns the  $Q$ -table via RUDDER’s  $Q$ -value estimation with  $\kappa$  correction (Type A variant ii from above). For BC+ $Q$  and DQfD a  $Q$ -table is learned by  $Q$ -learning. Hyperparameters were selected via grid search using the same amount of time for each method. See more details in appendix Section A.3. For different numbers of demonstrations, performance is measured by the number of episodes to achieve 80% of the average return of the demonstrations. A Wilcoxon rank-sum test determines the significance of performance differences between Align-RUDDER and the other methods.

**Task (I)** environment is a  $12 \times 12$  gridworld with four rooms. The target is in room #4 and the start is in room #1, which has 20 possible portal entry locations. For each episode the portal entry is indicated in the state. Figure 4 shows the number of episodes required for achieving 80% of the average reward of the demonstrations for different numbers of demonstrations. Results are averaged over 100 trials. **Align-RUDDER significantly outperforms all other methods, in particular with few demonstrations (with  $p$ -values  $< 10^{-10}$  for up to 10 demonstrations).**

**Task (II)** environment is a  $12 \times 24$  gridworld with eight rooms. The target is in room #8 and the start is in room #1, which has 20 possible portal entry locations. Figure 4 shows the results, where the settings and evaluation criteria are as in Task (I). **Align-RUDDER significantly outperforms all other methods, in particular with few demonstrations (with  $p$ -values  $< 10^{-26}$  for up to 10 demonstrations).**

**MineCraft.** We further test Align-RUDDER on the very challenging MineCraft ObtainDiamond task from the MineRL Minecraft dataset (Guss et al., 2019b). We do not use the intermediate rewards given by achieving sub-goals from the challenge, since Align-RUDDER is supposed to discover such sub-goals automatically via reward redistribution. In our setting, we only give reward for mining the diamond. Mining a diamond requires to gather resources and to build tools in a hierarchical way. To the best of our knowledge, no pure learning method (sub-goals are also learned) has mined a diamond yet (Scheller et al., 2020). The dataset contains demonstrations from human players. However, the



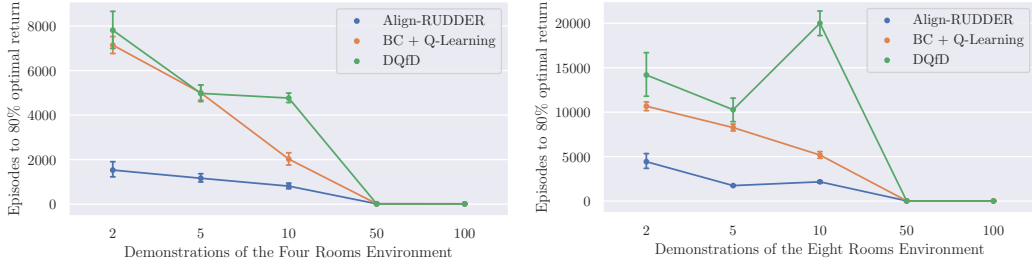


Figure 4: Comparison of Align-RUDDER and other methods on Task (I) (left) and Task (II) (right) with respect to the number of episodes required for learning on different numbers of demonstrations. Results are the average over 100 trials. In both tasks, Align-RUDDER significantly outperforms all other methods.

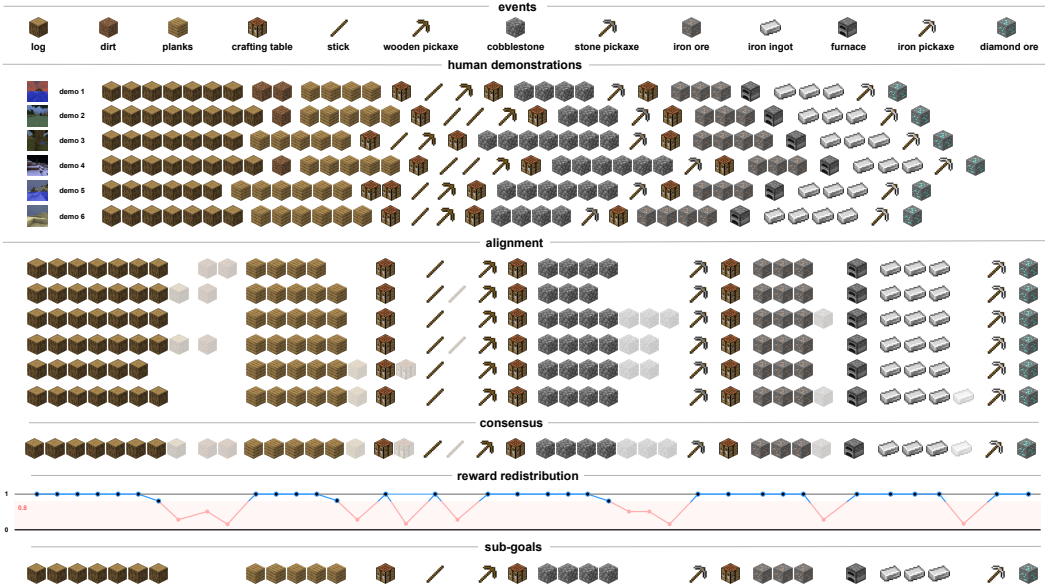


Figure 5: Example of alignment and reward redistribution for demonstrations of ObtainDiamond. Thresholding the redistributed reward identifies sub-goals.

number of demonstrations is insufficient to directly learn a policy from them that can mine a diamond (out of 117 demonstrations, 67 mined a diamond).

The implementation of the five steps of Align-RUDDER: (1) A state consists of two parts: a visual input and an inventory (including the equip state). Both parts are scaled to have the same information, that is, the same number of components and the same variance. We cluster the differences of consecutive states according to "Explaining Away Problem" in [Arjona-Medina et al. \(2019\)](#). We removed very large clusters and merged small clusters to have about 20 clusters corresponding to events, which are characterized by inventory changes. Finally, demonstrations are mapped to sequences of events. (2) The scoring matrix is computed according to Eq. (3). (3) The 10 shortest demonstrations that received a diamond are aligned by ClustalW with gap penalties set to zero and no biological options. (4) A profile model and a PSSM is extracted from the multiple alignment. (5) Reward is redistributed according to the differences of profile alignment scores of consecutive sub-sequences according to Eq. (5) using the PSSM from step (4).

Based on the reward redistribution, we define sub-goals. Sub-goals are identified as profile model positions which obtain an average redistributed reward above a threshold for the demonstrations. Demonstration sub-sequences between sub-goals are considered as demonstrations for the sub-tasks. New sub-sequences that are generated by the agent are aligned to the profile model to determine

whether a sub-goal is achieved. The redistributed reward between sub-goals is given at the end of the sub-sequence, therefore, the sub-tasks have also episodic reward. Figure 5 shows how sub-goals are identified using reward redistribution. Sub-agents are first pre-trained on the demonstrations for the sub-tasks using Behavioral Cloning, and further trained in the environment using Proximal Policy Optimization (PPO) (Schulman et al., 2018).

Our main agent can perform all actions but additionally can execute sub-agents and learns via the redistributed reward (return-equivalent MDP). The main agent is initialized by executing sub-agents according to the alignment but can deviate from this strategy. More information about architectures, hyperparameters and other implementation details can be found in the Appendix. Using only 10 demonstrations, Align-RUDDER is able to learn to mine a diamond. A diamond is obtained in 0.1% of the cases considering the 31 extracted sub-tasks from the ObtainDiamond environment. To put this percentage in context, assume a 0.5 probability of success for every extracted sub-task, which already requires a pretty skilled agent. The resulting success rate for mining the diamond would be approximately  $4.66 \times 10^{-10}$ .

**Conclusions.** We have introduced Align-RUDDER that can learn to solve highly complex tasks with delayed and sparse reward from few demonstrations. Align-RUDDER is based on the theory of reward redistribution, which guarantees that optimal policies are kept, while the delay of the reward is considerably reduced. Reward redistribution utilizes alignment techniques from bioinformatics. Align-RUDDER outperforms competitors on artificial tasks with few demonstrations. On the MineCraft ObtainDiamond task, Align-RUDDER was able to mine a diamond in 0.1% of the cases.

#### ACKNOWLEDGMENTS

The ELLIS Unit Linz, the LIT AI Lab, the Institute for Machine Learning, are supported by the Federal State Upper Austria. IARAI is supported by Here Technologies. We thank the projects AI-MOTION (LIT-2018-6-YOU-212), DeepToxGen (LIT-2017-3-YOU-003), AI-SNN (LIT-2018-6-YOU-214), DeepFlood (LIT-2019-8-YOU-213), Medical Cognitive Computing Center (MC3), PRIMAL (FFG-873979), S3AI (FFG-872172), DL for granular flow (FFG-871302), ELISE (H2020-ICT-2019-3 ID: 951847), AIDD (MSCA-ITN-2020 ID: 956832). We thank Janssen Pharmaceutica, UCB Biopharma SRL, Merck Healthcare KGaA, Audi.JKU Deep Learning Center, TGW LOGISTICS GROUP GMBH, Silicon Austria Labs (SAL), FILL Gesellschaft mbH, Anyline GmbH, Google Brain, ZF Friedrichshafen AG, Robert Bosch GmbH, Software Competence Center Hagenberg GmbH, TÜV Austria, and the NVIDIA Corporation.

#### REFERENCES

- P. Abbeel and A. Y. Ng. Apprenticeship learning via inverse reinforcement learning. In *Proceedings of the Twenty-First International Conference on Machine Learning*, pp. 1, 2004. ISBN 1581138385.
- S. F. Altschul, W. Gish, W. Miller, E. W. Myers, and D. J. Lipman. Basic local alignment search tool. *J. Molec. Biol.*, 214:403–410, 1990.
- S. F. Altschul, T. L. Madden, A. A. Schäffer, J. Zhang, Z. Zhang, W. Miller, and D. J. Lipman. Gapped BLAST and PSI-BLAST: a new generation of protein database search programs. *Nucleic Acids Research*, 25(17):3389–3402, 1997. doi: 10.1093/nar/25.17.3389.
- J. A. Arjona-Medina, M. Gillhofer, M. Widrich, T. Unterthiner, J. Brandstetter, and S. Hochreiter. RUDDER: return decomposition for delayed rewards. In *Advances in Neural Information Processing Systems 32*, pp. 13566–13577, 2019.
- A. Bairoch and P. Bucher. PROSITE: recent developments. *Nucleic acids research*, 22(17):3583–9, 1994.
- A. Barreto, W. Dabney, R. Munos, J. Hunt, T. Schaul, H. P. vanHasselt, and D. Silver. Successor features for transfer in reinforcement learning. In *Advances in Neural Information Processing Systems 30*, pp. 4055–4065, 2017. ArXiv 1606.05312.
- Y. Bengio and Y. Lecun. *Large-scale kernel machines*, chapter Scaling learning algorithms towards AI, pp. 321–359. MIT Press, 2007.

- 
- A. Billard, S. Calinon, R. Dillmann, and S. Schaal. Robot programming by demonstration. In B. Siciliano and O. Khatib (eds.), *Springer Handbook of Robotics*, pp. 1371–1394. Springer, 2008.
- T. Brys, A. Harutyunyan, H. B. Suay, S. Chernova, M. E. Taylor, and A. Nowé. Reinforcement learning from demonstration through shaping. In *Proc. of the 24th Int. Joint Conf. on Artificial Intelligence, (IJCAI’15)*, pp. 3352–3358, 2015.
- K. Chao and L. Zhang. *Sequence comparison: theory and methods*. Springer, 2009. ISBN 9781848003200.
- P. J. A. Cock, T. Antao, J. T. Chang, B. A. Chapman, C. J. Cox, A. Dalke, I. Friedberg, T. Hamelryck, F. Kauff, B. Wilczynski, and M. J. L. de Hoon. Biopython: freely available Python tools for computational molecular biology and bioinformatics. *Bioinformatics*, 25(11):1422–1423, 03 2009. ISSN 1367-4803. doi: 10.1093/bioinformatics/btp163.
- F. Corpet. Multiple sequence alignment with hierarchical clustering. *Nucleic Acids Research*, 16(22): 10881–10890, 1988.
- P. Dayan. Improving generalization for temporal difference learning: The successor representation. *Neural Computation*, 5(4):613–624, 1993.
- M. O. Dayhoff. *Atlas of Protein Sequence and Structure*, volume 3. Silver Spring, 1978.
- Y. Duan, M. Andrychowicz, B. C. Stadie, J. Ho, J. Schneider, I. Sutskever, P. Abbeel, and W. Zaremba. One-shot imitation learning. In *Advances in Neural Information Processing Systems 30*, pp. 1087–1098, 2017.
- A. Ecoffet, J. Huizinga, J. Lehman, K. O. Stanley, and J. Clune. Go-Explore: A new approach for hard-exploration problems. *arXiv*, abs/1901.10995, 2019.
- R. C. Edgar. MUSCLE: multiple sequence alignment with high accuracy and high throughput. *Nucleic Acids Research*, 32(5):1792–1797, 2004.
- L. Espeholt, H. Soyer, R. Munos, K. Simonyan, V. Mnih, T. Ward, Y. Doron, V. Firoiu, T. Harley, I. Dunning, S. Legg, and K. Kavukcuoglu. IMPALA: Scalable distributed Deep-RL with importance weighted actor-learner architectures. In J. Dy and A. Krause (eds.), *Proceedings of the 35th International Conference on Machine Learning*, 2018. ArXiv: 1802.01561.
- B. Eysenbach, R. Salakhutdinov, and S. Levine. Search on the replay buffer: Bridging planning and reinforcement learning. In *Advances in Neural Information Processing Systems 32*, pp. 15220–15231, 2019.
- C. Finn, T. Yu, T. Zhang, P. Abbeel, and S. Levine. One-shot visual imitation learning via meta-learning. In *1st Annual Conference on Robot Learning (CoRL)*, volume 78 of *Proceedings of Machine Learning Research*, pp. 357–368. PMLR, 2017.
- B. J. Frey and D. Dueck. Clustering by passing messages between data points. *Science*, 315(5814): 972–976, 2007. doi: 10.1126/science.1136800.
- O. Gotoh. An improved algorithm for matching biological sequences. *Journal of Molecular Biology*, 162(3):705–708, 1982.
- W. H. Guss, C. Codel, K. Hofmann, B. Houghton, N. Kuno, S. Milani, S. P. Mohanty, D. P. Liebana, R. Salakhutdinov, N. Topin, M. Veloso, and P. Wang. The MineRL competition on sample efficient reinforcement learning using human priors. *arXiv*, 2019a.
- W. H. Guss, B. Houghton, N. Topin, P. Wang, C. Codel, M. Veloso, and R. Salakhutdinov. MineRL: A large-scale dataset of Minecraft demonstrations. In *Proc. of the 28th Int. Joint Conf. on Artificial Intelligence (IJCAI’19)*, 2019b.
- S. Henikoff and J. G. Henikoff. Amino acid substitution matrices from protein blocks. *Proceedings of the National Academy of Sciences of the United States of America*, 89(22):10915–10919, 1992.

- 
- T. Hester, M. Vecerík, O. Pietquin, M. Lanctot, T. Schaul, B. Piot, A. Sendonaris, G. Dulac-Arnold, I. Osband, J. Agapiou, J. Z. Leibo, and A. Gruslys. Learning from demonstrations for real world reinforcement learning. *ArXiv*, 2017.
- T. Hester, M. Vecerík, O. Pietquin, M. Lanctot, T. Schaul, B. Piot, D. Horgan, J. Quan, A. Sendonaris, I. Osband, G. Dulac-Arnold, J. Agapiou, J. Z. Leibo, and A. Gruslys. Deep q-learning from demonstrations. In *The Thirty-Second AAAI Conference on Artificial Intelligence (AAAI-18)*. Association for the Advancement of Artificial Intelligence, 2018.
- D. S. Hirschberg. A linear space algorithm for computing maximal common subsequences. *Communications of the ACM*, 18(6):341–343, 1975. doi: 10.1145/360825.360861.
- J. Ho and S. Ermon. Generative adversarial imitation learning. In *Advances in Neural Information Processing Systems 29*, pp. 4565–4573, 2016.
- S. Hochreiter and J. Schmidhuber. Long short-term memory. Technical Report FKI-207-95, Fakultät für Informatik, Technische Universität München, 1995.
- S. Hochreiter and J. Schmidhuber. Long short-term memory. *Neural Comput.*, 9(8):1735–1780, 1997a.
- S. Hochreiter and J. Schmidhuber. LSTM can solve hard long time lag problems. In M. C. Mozer, M. I. Jordan, and T. Petsche (eds.), *Advances in Neural Information Processing Systems 9*, pp. 473–479, Cambridge, MA, 1997b. MIT Press.
- I. A. Hosu and T. Rebedea. Playing Atari games with deep reinforcement learning and human checkpoint replay. *ArXiv*, 2016.
- H. Daumé III, J. Langford, and D. Marcu. Search-based structured prediction, 2009.
- M. Jing, X. Ma, W. Huang, F. Sun, C. Yang, B. Fang, and H. Liu. Reinforcement learning from imperfect demonstrations under soft expert guidance. *ArXiv*, abs/1911.07109, 2019.
- K. Judah, A. P. Fern, T. G. Dietterich, and P. Adepalli. Active imitation learning: Formal and practical reductions to i.i.d. learning. *J. Mach. Learn. Res.*, 15(1):3925–3963, 2014. ISSN 1532-4435.
- S. Kakade and J. Langford. Approximately optimal approximate reinforcement learning. In *19th International Conference on Machine Learning (ICML)*, pp. 267–274, 2002.
- S. Karlin and S. F. Altschul. Methods for assessing the statistical significance of molecular sequence features by using general scoring schemes. *Proceedings of the National Academy of Sciences of the United States of America*, 87(6):2264–2268, 1990. doi: 10.1073/pnas.87.6.2264.
- S. Karlin, A. Dembo, and T. Kawabata. Statistical composition of high-scoring segments from molecular sequences. *Ann. Statist.*, 18(2):571–581, 1990. doi: 10.1214/aos/1176347616.
- R. Khardon. Learning to take actions. *Machine Learning*, 35(1):57–90, 1999.
- B. Kim, A. Farahmand, J. Pineau, and D. Precup. Learning from limited demonstrations. In *Advances in Neural Information Processing Systems 26*, 2013.
- A. S. Lakshminarayanan, S. Ozair, and Y. Bengio. Reinforcement learning with few expert demonstrations. In *NIPS Workshop on Deep Learning for Action and Interaction*, 2016.
- H. M. Le, N. Jiang, A. Agarwal, M. Dudík, Y. Yue, and H. Daumé III. Hierarchical imitation and reinforcement learning. In *Proceedings of the 35th International Conference on Machine Learning (ICML)*, volume 80 of *Proceedings of Machine Learning Research*, pp. 2923–2932, 2018.
- M. Lopes, F. S. Melo, and L. Montesano. Active learning for reward estimation in inverse reinforcement learning. In *European Conference on Machine Learning and Knowledge Discovery in Databases (ECML/PKDD)*, volume 5782 of *Lecture Notes in Computer Science*, pp. 31–46. Springer, 2009.
- J. Luoma, S. Ruutu, A. W. King, and H. Tikkanen. Time delays, competitive interdependence, and firm performance. *Strategic Management Journal*, 38(3):506–525, 2017. doi: 10.1002/smj.2512.

- 
- M. Machado, C. Rosenbaum, X. Guo, M. Liu, G. Tesauro, and M. Campbell. Eigenoption discovery through the deep successor representation. *arXiv*, abs/1710.11089, 2017.
- J. A. Mccammon and P. G. Wolynes. Highly specific protein sequence motifs for genome analysis. *Computational Biomolecular Science*, 95(May):5865–5871, 1998.
- D. Michie and R. Camacho. *Building Symbolic Representations of Intuitive Real-Time Skills from Performance Data*, pp. 385–418. Oxford University Press, Inc., USA, 1994. ISBN 0198538502.
- D. Michie, M. Bain, and J. Hayes-Michie. *Cognitive models from subcognitive skills*, pp. 71–99. Control, Robotics and Sensors. Institution of Engineering and Technology, 1990. doi: 10.1049/PBCE044E\_ch5.
- B. Morgenstern. DIALIGN: Multiple DNA and protein sequence alignment at BiBiServ. *Nucleic Acids Research*, 32:W33–6, 2004.
- A. Nair, B. McGrew, M. Andrychowicz, W. Zaremba, and P. Abbeel. Overcoming exploration in reinforcement learning with demonstrations. In *2018 IEEE International Conference on Robotics and Automation, ICRA 2018, Brisbane, Australia, May 21-25, 2018*, pp. 6292–6299. IEEE, 2018.
- S. B. Needleman and C. D. Wunsch. A general method applicable to the search for similarities in the amino acid sequence of two proteins. *Journal of Molecular Biology*, 48(3):443–453, 1970.
- A. Y. Ng and S. J. Russell. Algorithms for inverse reinforcement learning. In *Proceedings of the Seventeenth International Conference on Machine Learning*, pp. 663–670, 2000. ISBN 1558607072.
- C. Notredame, D. G. Higgins, and J. Heringa. T-coffee: a novel method for fast and accurate multiple sequence alignment. *Journal of Molecular Biology*, 302(1):205–217, 2000.
- D. A. Pomerleau. Efficient training of artificial neural networks for autonomous navigation. *Neural Comput.*, 3(1):88–97, 1991. ISSN 0899-7667.
- M. L. Puterman. *Markov Decision Processes*. John Wiley & Sons, Inc., 2nd edition, 2005. ISBN 978-0-471-72782-8.
- H. Rahmandad, N. Repenning, and J. Sterman. Effects of feedback delay on learning. *System Dynamics Review*, 25(4):309–338, 2009. doi: 10.1002/sdr.427.
- A. Rajeswaran, V. Kumar, A. Gupta, G. Vezzani, J. Schulman, E. Todorov, and S. Levine. Learning complex dexterous manipulation with deep reinforcement learning and demonstrations. In *Robotics: Science and Systems XIV*, 2018.
- R. Ramesh, M. Tomar, and B. Ravindran. Successor options: An option discovery framework for reinforcement learning. In *Proc. of the 28th Int. Joint Conf. on Artificial Intelligence (IJCAI’19)*, 2019.
- S. Reddy, A. D. Dragan, and S. Levine. SQIL: imitation learning via regularized behavioral cloning. *ArXiv*, 2020. Eighth International Conference on Learning Representations (ICLR).
- D. Rolnick, A. Ahuja, J. Schwarz, T. P. Lillicrap, and G. Wayne. Experience replay for continual learning. In *Advances in Neural Information Processing Systems 32*, pp. 348–358, 2019.
- S. Ross and D. Bagnell. Efficient reductions for imitation learning. In *Proceedings of the Thirteenth International Conference on Artificial Intelligence and Statistics*, volume 9 of *Proceedings of Machine Learning Research*, pp. 661–668, 2010.
- S. Ross, G. Gordon, and D. Bagnell. A reduction of imitation learning and structured prediction to no-regret online learning. In *Proceedings of the Fourteenth International Conference on Artificial Intelligence and Statistics*, volume 15 of *Proceedings of Machine Learning Research*, pp. 627–635, 2011.
- S. Schaal. Learning from demonstration. In *Proceedings of the 9th International Conference on Neural Information Processing Systems (NIPS’96)*, pp. 1040–1046, Cambridge, MA, USA, 1996. MIT Press.



- 
- C. Scheller, Y. Schraner, and M. Vogel. Sample efficient reinforcement learning through learning from demonstrations in Minecraft. *arXiv*, abs/2003.06066, 2020.
- J. Schulman, F. Wolski, P. Dhariwal, A. Radford, and O. Klimov. Proximal policy optimization algorithms. *ArXiv*, 2018.
- F. Sievers, A. Wilm, D. Dineen, T. J. Gibson, K. Karplus, W. Li, R. Lopez, H. McWilliam, M. Remmert, J. Soding, J. D. Thompson, and D. G. Higgins. Fast, scalable generation of high-quality protein multiple sequence alignments using Clustal Omega. *Molecular Systems Biology*, 7(1): 539–539, 2014.
- Jr. A. R. Silva, V. Grassi, and D. F. Wolf. Continuous deep maximum entropy inverse reinforcement learning using online POMDP. In *19th International Conference on Advanced Robotics (ICAR)*, pp. 382–387. IEEE, 2019.
- D. Silver, A. Huang, C. J. Maddison, A. Guez, L. Sifre, G. van den Driessche, J. Schrittwieser, I. Antonoglou, V. Panneershelvam, M. Lanctot, S. Dieleman, D. Grewe, J. Nham, N. Kalchbrenner, I. Sutskever, T. P. Lillicrap, M. Leach, K. Kavukcuoglu, T. Graepel, and D. Hassabis. Mastering the game of Go with deep neural networks and tree search. *Nature*, 529(7587):484–489, 2016. doi: 10.1038/nature16961.
- D. Silver, T. Hubert, J. Schrittwieser, I. Antonoglou, M. Lai, A. Guez, M. Lanctot, L. Sifre, D. Kumaran, T. Graepel, T. P. Lillicrap, K. Simonyan, and D. Hassabis. Mastering Chess and Shogi by self-play with a general reinforcement learning algorithm. *ArXiv*, 2017.
- A. Skrynnik, A. Staroverov, E. Aitygulov, K. Aksenov, V. Davydov, and A. I. Panov. Hierarchical deep q-network with forgetting from imperfect demonstrations in Minecraft. *arXiv*, abs/1912.08664, 2019.
- T. F. Smith and M. S. Waterman. Identification of common molecular subsequences. *Journal of Molecular Biology*, 147(1):195–197, 1981.
- G. D. Stormo, T. D. Schneider, L. Gold, and A. Ehrenfeucht. Use of the 'Perceptron' algorithm to distinguish translational initiation sites in E. coli. *Nucleic Acids Research*, 10(9):2997–3011, 1982.
- H. B. Suay, T. Brys, M. E. Taylor, and S. Chernova. Learning from demonstration for shaping through inverse reinforcement learning. In *Proceedings of the 2016 International Conference on Autonomous Agents & Multiagent Systems*, pp. 429–437. ACM, 2016.
- K. Subramanian, C. L. Isbell, and A. L. Thomaz. Exploration from demonstration for interactive reinforcement learning. In *Proceedings of the 2016 International Conference on Autonomous Agents & Multiagent Systems*, pp. 447–456, 2016.
- W. Sun, A. Venkatraman, G. J. Gordon, B. Boots, and J. A. Bagnell. Deeply AggreVaTeD: Differentiable imitation learning for sequential prediction. In *Proceedings of the 34th International Conference on Machine Learning*, volume 70 of *Proceedings of Machine Learning Research*, pp. 3309–3318. PMLR, 2017.
- W. Sun, J.A. Bagnell, and B. Boots. Truncated horizon policy search: Combining reinforcement learning & imitation learning. In *6th International Conference on Learning Representations, ICLR 2018, Vancouver, BC, Canada, April 30 - May 3, 2018, Conference Track Proceedings*, 2018.
- R. S. Sutton and A. G. Barto. *Reinforcement Learning: An Introduction*. MIT Press, Cambridge, MA, 2 edition, 2018.
- R. S. Sutton, D. Precup, and S. P. Singh. Between MDPs and Semi-MDPs: A framework for temporal abstraction in reinforcement learning. *Artificial Intelligence*, 112(1-2):181–211, 1999.
- U. Syed and R. E. Schapire. A game-theoretic approach to apprenticeship learning. In *Advances in Neural Information Processing Systems 20*, 2007.
- M. E. Taylor, H. B. Suay, and S. Chernova. Integrating reinforcement learning with human demonstrations of varying ability. In *10th International Conference on Autonomous Agents and Multiagent Systems (AAMAS 2011), Taipei, Taiwan, May 2-6, 2011, Volume 1-3*, pp. 617–624, 2011.

- 
- J. D. Thompson, D. G. Higgins, and T. J. Gibson. CLUSTAL W: improving the sensitivity of progressive multiple sequence alignment through sequence weighting, position-specific gap penalties and weight matrix choice. *Nucleic Acids Research*, 22(22):4673–4680, 1994.
- A. Tucker, A. Gleave, and S. Russell. Inverse reinforcement learning for video games. *arXiv*, 2018.
- M. Vecerík, T. Hester, J. Scholz, F. Wang, O. Pietquin, B. Piot, N. Heess, T. Rothörl, T. Lampe, and M. A. Riedmiller. Leveraging demonstrations for deep reinforcement learning on robotics problems with sparse rewards. *ArXiv*, abs/1707.08817, 2017.
- L. Wang and T. Jiang. On the Complexity of Multiple Sequence Alignment. *Journal of Computational Biology*, 1(4):337–348, 1994.
- X. Zhang and H. Ma. Pretraining deep actor-critic reinforcement learning algorithms with expert demonstrations. *ArXiv*, abs/1801.10459, 2018.
- A. Zhou, E. Jang, D. Kappler, A. Herzog, M. Khansari, P. Wohlhart, Y. Bai, M. Kalakrishnan, S. Levine, and C. Finn. Watch, try, learn: Meta-learning from demonstrations and rewards. In *International Conference on Learning Representations*, 2020.
- B. D. Ziebart, A. Maas, J. A. Bagnell, and A. K. Dey. Maximum entropy inverse reinforcement learning. In *Proceedings of the 23rd National Conference on Artificial Intelligence - Volume 3*, AAAI’08, pp. 1433–1438. AAAI Press, 2008. ISBN 9781577353683.

---

## A APPENDIX

### CONTENTS OF THE APPENDIX

A.1 Introduction to the Appendix . . . . .	16
A.2 Sequence Alignment . . . . .	16
A.3 Artificial Task Experiments . . . . .	18
A.3.1 Hyperparameter Selection . . . . .	18
A.3.2 Figures . . . . .	18
A.3.3 Artificial Task $p$ -values . . . . .	19
A.4 Minecraft Experiments . . . . .	20
A.4.1 MineCraft . . . . .	20
A.4.2 Related Work and Steps Towards a General Agent . . . . .	20
A.4.3 Implementation of our Algorithm for Minecraft . . . . .	21
A.4.4 Policy and Value Network Architecture . . . . .	23
A.4.5 Imitation Learning of Sub-Task Agents . . . . .	24
A.4.6 Reinforcement Learning on Sub-Task Agents . . . . .	25

### LIST OF FIGURES

A.1 Clusters formed in the FourRooms and EightRooms environment . . . . .	18
A.2 FourRooms and EightRooms environments . . . . .	19
A.3 Reward redistribution for the FourRooms and EightRooms environments . . . . .	19
A.4 Conceptual overview of our MineRL agent . . . . .	21
A.5 Mapping of clusters to letters . . . . .	22
A.6 Comparing the consensus frequencies of BC, Align-Rudder, and humans . . . . .	22
A.7 Trajectory replay given by an exemplary consensus . . . . .	23
A.8 Conceptual architecture of Align-RUDDER MineRL policy and value networks . . . . .	23
A.9 Discretization and interpolation of camera angles . . . . .	24

#### A.1 INTRODUCTION TO THE APPENDIX

This is the appendix to the paper “Align-RUDDER: Learning from few Demonstrations by Reward Redistribution”. The appendix aims at supporting the main document and provides more detailed information about the implementation of our method for different tasks. The content of this document is summarized as follows:

- Section A.2 provides a brief overview of sequence alignment methods and the hyperparameters used in our experiments.
- Section A.3 provides figures and tables to support the results of the experiments in Artificial Tasks (I) and (II).
- Section A.4 explains in detail the experiments conducted in the Minecraft *ObtainDiamond* task.

#### A.2 SEQUENCE ALIGNMENT

In bioinformatics, sequence alignment identifies regions of significant similarity among different biological sequences to establish evolutionary relationships between those sequences. In 1970, Needleman and Wunsch proposed a global alignment method based on dynamic programming (Needleman & Wunsch, 1970). This approach ensures the best possible alignment given a substitution matrix, such as PAM (Dayhoff, 1978) or BLOSUM (Henikoff & Henikoff, 1992), and other parameters to penalize gaps in the alignment. This method is of  $O(mn)$  complexity both in memory and time, which could be prohibitive in long sequences like genomes. An optimization of this method was carried out by Dan Hirschberg, using less memory of  $O(m + n)$ , but still requiring  $O(mn)$  runtime (Hirschberg, 1975).

Later, Smith and Waterman developed a local alignment method for sequences (Smith & Waterman, 1981). It is a variation of Needleman and Wunsch’s method, keeping the substitution matrix and the gap-scoring scheme but setting cells in the similarity matrix with negative scores to zero. The complexity for this algorithm is of  $O(n^2M)$ . Osamu Gotoh published an optimization of this method, running in  $O(mn)$  runtime (Gotoh, 1982).

---

The main difference between both methods is the following:

- The global alignment method by Needleman and Wunsch aligns the sequences fixing the first and the last position of both sequences. It attempts to align every symbol in the sequence, allowing some gaps, but the main purpose is to get a global alignment. This is especially useful when the two sequences are highly similar. For instance:

```
ATCGGATCGACTGGCTAGATCATCGCTGG
CGAGCATC-ACTGTCT-GATCGACCTTAG
*  ***  *****  **  *****  *  *  *
```

- As an alternative to global methods, the local method of Smith and Waterman aligns the sequences with a higher degree of freedom, allowing the alignment to start or end with gaps. This is extremely useful when the two sequences are substantially dissimilar in general but suspected of having a highly related sub region.

```
ATCAAGGAGATCATCGCTGGACTGAGTGGCT----ACGTGGTATGT
ATC----CGATCATCGCTGG-CTGATCGACCTTCTACGT-----
***          *****          *****  *  *          *****
```

**A.2.0.1 Multiple Sequence Alignment algorithms.** The sequence alignment algorithms by Needleman and Wunsch and Smith and Waterman are limited to aligning two sequences. The approaches for generalizing these algorithms to multiple sequences can be classified into four categories:

- Exact methods ([Wang & Jiang, 1994](#)).
- Progressive methods: ClustalW ([Thompson et al., 1994](#)), Clustal Omega ([Sievers et al., 2014](#)), T-Coffee ([Notredame et al., 2000](#)).
- Iterative and search algorithms: DIALIGN ([Morgenstern, 2004](#)), MultiAlign ([Corpet, 1988](#)).
- Local methods: eMOTIF ([Mccammon & Wolynes, 1998](#)), PROSITE ([Bairoch & Bucher, 1994](#)).

For more details, visit *Sequence Comparison: Theory and methods* ([Chao & Zhang, 2009](#)).

In our experiments, we use ClustalW from Biopython ([Cock et al., 2009](#)) with the following parameters:

```
clustalw2 -ALIGN -CLUSTERING=UPGMA -NEGATIVE " \
"-INFILE={infile} -OUTFILE={outfile} " \
"-PWMATRIX={scores} -PWGAPOPEN=0 -PWGAPEXT=0 " \
"-MATRIX={scores} -GAPOPEN=0 -GAPEXT=0 -CASE=UPPER " \
"-NOPGAP -NOHGAP -MAXDIV=0 -ENDGAPS -NOVGAP " \
"-NEWTREE={outputtree} -TYPE=PROTEIN -OUTPUT=GDE
```

where the PWMATRIX and MATRIX are computed according to step (II) in Sec. [Reward Redistribution by Sequence Alignment](#) of the main paper.

### A.3 ARTIFICIAL TASK EXPERIMENTS

This section provides additional information that supports the results reported in the main paper for Artificial Tasks (I) and (II).

#### A.3.1 HYPERPARAMETER SELECTION

For (BC)+ $Q$ -Learning and Align-RUDDER, we performed a grid search to select the learning rate from the following values  $[0.1, 0.05, 0.01]$ . We used 20 different seeds for each value and each number of demonstrations and then selected the setting with the highest success for all number of demonstrations. The final learning rate for (BC)+ $Q$ -Learning and DQfD is 0.01 and for Align-RUDDER it is 0.1.

For DQfD, we set the experience buffer size to 30,000 and the number of experiences sampled at every timestep to 10. The DQfD loss weights are set to 0.01, 0.01 and 1.0 for the  $Q$ -learning loss term,  $n$ -step loss term and the expert loss respectively during pre-training. During online learning, we change the loss terms to 1.0, 1.0 and 0.01 for the  $Q$ -learning loss term,  $n$ -step loss term and the expert loss term. This was necessary to enable faster learning for DQfD. The expert action margin is 0.8.

For successor representation, we use a learning rate of 0.1 and a gamma of 0.99. We update the successor table multiple times using the same transition (state, action, next state) from the demonstration.

For affinity propagation, we use a damping factor of 0.5 and set the maximum number of iterations to 1000. Furthermore, if we obtain more than 15 clusters we combine clusters based on the similarity of the cluster centers.

#### A.3.2 FIGURES

Figure A.2 shows sample trajectories in the FourRooms and EightRooms environment, with the initial and target positions marked in red and green respectively. Figure A.1 shows the clusters after performing clustering with Affinity Propagation. Different colors indicate different clusters. Figure A.3 shows the reward redistribution for the given example trajectories in the FourRooms and EightRooms environments.

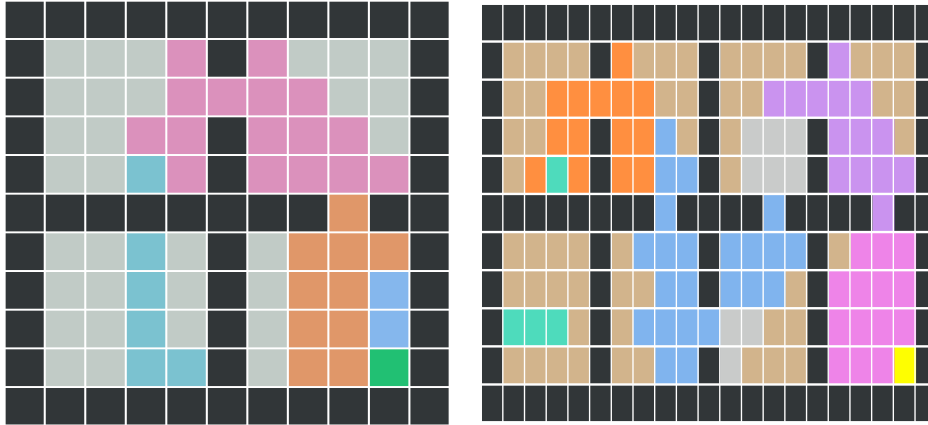


Figure A.1: Clusters formed in the FourRooms (left) and EightRooms (right) environment after performing clustering with Affinity Propagation using the successor representation with 10 demonstrations. Different colors represent different clusters.



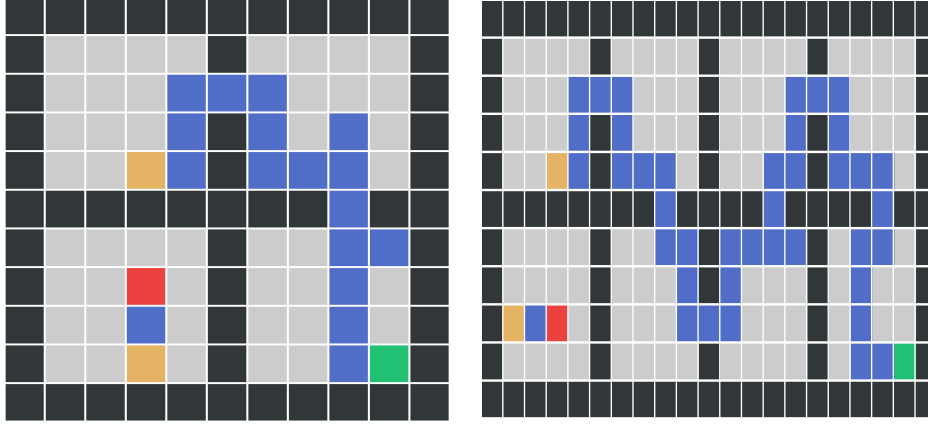


Figure A.2: FourRooms (left) and EightRooms (right) environments. Initial position is indicated in red, the portal between the first and second room in yellow and the goal in green.

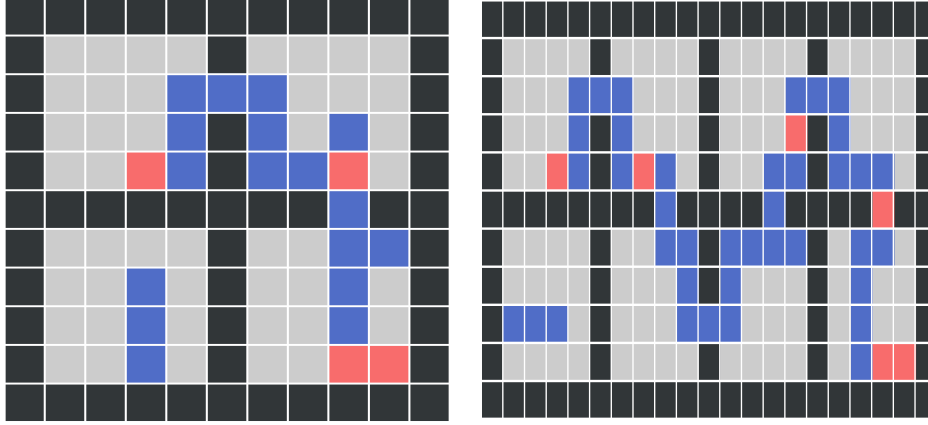


Figure A.3: Reward redistribution for the above trajectories in the FourRooms (left) and EightRooms (right) environments.

### A.3.3 ARTIFICIAL TASK $p$ -VALUES

Tables A.1 and A.2 show the  $p$ -values obtained by performing a Mann-Whitney-U test between Align-RUDDER and BC+ $Q$ -Learning and DQfD respectively.

	2	5	10	50	100
Align-RUDDER vs. BC+ $Q$ -Learn.	8.8361e-31	2.8198e-30	1.1380e-09	0.3547	0.1558
Align-RUDDER vs. DQfD	2.6984e-29	4.3348e-30	1.3456e-32	1.0000	0.9999

Table A.1:  $p$ -values for Artificial Task (I), FourRooms, obtained by performing a Mann-Whitney-U test.

	2	5	10	50	100
Align-RUDDER vs. BC+Q-Learn.	4.5409e-20	1.2776e-34	4.8883e-25	0.3730	0.6096
Align-RUDDER vs. DQfD	1.2202e-08	8.9356e-20	5.6255e-31	0.9999	0.9964

Table A.2:  $p$ -values for Artificial Task (II), EightRooms, obtained by performing a Mann-Whitney-U test.

#### A.4 MINECRAFT EXPERIMENTS

In this section we explain in detail the implementation of Align-RUDDER for solving the task *ObtainDiamond*.

##### A.4.1 MINECRAFT

We show that our approach can be applied to complex tasks by evaluating it on the MineRL Minecraft dataset (Guss et al., 2019b). This dataset provides a large collection of demonstrations from human players solving six different tasks in the sandbox game Minecraft. In addition to the human demonstrations the MineRL dataset also provides an OpenAI-Gym wrapper for Minecraft. The dataset includes demonstrations for the following tasks:

- navigating to target location following a compass,
- collecting wood by chopping trees,
- obtaining an item by collecting resources and crafting, and
- free play "survival" where the player is free to choose his own goal.

The demonstrations include the video showing the players' view (without user interface), the players' inventory at every time step and the actions performed by the player. We focus on the third task of obtaining a target item, namely a diamond. This task is very challenging as it is necessary to obtain several different resources and tools and has been the focus of a challenge (Guss et al., 2019a) at NeurIPS' 19. By the end of this challenge no entry was able to obtain the diamond.

We show that our method is well suited for solving the task of obtaining the diamond, which can be decomposed into sub-tasks by reward redistribution after aligning successful demonstrations.

##### A.4.2 RELATED WORK AND STEPS TOWARDS A GENERAL AGENT

In the following, we review two approaches Skrynnik et al. (2019); Scheller et al. (2020) where more details are available and compare them with our approach.

Skrynnik et al. (2019) address the problem with a TD based hierarchical Deep  $Q$ -Network (DQN) and by utilizing the hierarchical structure of expert trajectories by extracting sequences of meta-actions and sub-goals. This approach allowed them to achieve the 1st place in the official NeurIPS' 19 MineRL challenge (Skrynnik et al., 2019). In terms of pre-processing, our approaches have in common that both rely on frame skipping and action space discretization. However, they reduce the action space to ten distinct joint environment actions (e.g. *move camera & attack*) and treat inventory actions separately by executing a sequence of semantic actions. We aim at taking a next step towards a more general agent by introducing an action space preserving the agent's full freedom of action in the environment (more details are provided below). This allows us to avoid the distinction between item (environment) and semantic (inventory) agents and to train identically structured agents in the same fashion regardless of facing a mining, crafting, placing or smelting sub-task. Skrynnik et al. (2019) extract a sub-task chain by separately examining each expert trajectory and by considering the time of appearance of items in the inventory in chronological order. For agent training their approach follows a heuristic where they distinguish between collecting the item *log* and all remaining items. The *log*-agent is trained by starting with the *TreeChop* expert trajectories and then gradually injecting trajectories collected from interactions with the environment into the DQN's replay buffer. For the remaining items they rely on the expert data of *ObtainIronPickaxeDense* and imitation learning. Given our proposed sequence alignment and reward redistribution methodology we are able to avoid this shift in training paradigm and to leverage all available training data (*ObtainDiamond*,

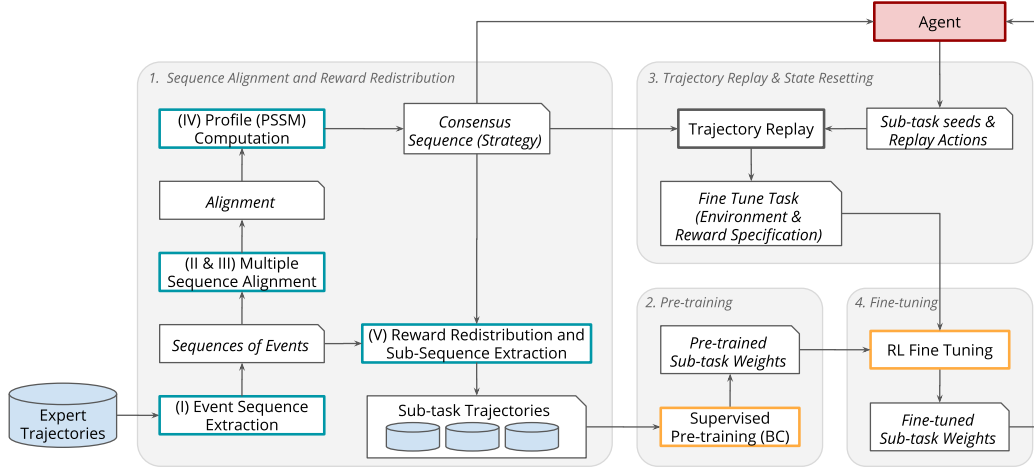


Figure A.4: Conceptual overview of our MineRL agent.

*ObtainIronPickaxe* and *TreeChop*) at the same time. In short, we collect all expert trajectories in one pool, perform sequence alignment yielding a common diamond consensus along with the corresponding reward redistribution and the respective sub-task sequences. Given this restructuring of the problem into local sub-problems with redistributed reward all sub-task agents are then trained in the same fashion (e.g. imitation learning followed by RL-based fine-tuning). Reward redistribution guarantees that the optimal policies are preserved (Arjona-Medina et al., 2019).

Scheller et al. (2020) achieved the 3rd place on the official leader board following a different line of research and addressed the problem with a single *end-to-end* off-policy IMPALA (Espeholt et al., 2018) actor-critic agent, again utilizing experience replay to incorporate the expert data (Scheller et al., 2020). To prevent catastrophic forgetting of the behavior for later, less frequent sub-tasks they introduce value clipping and apply CLEAR (Rolnick et al., 2019) to both, policy and value networks. Treating the entire problem as a whole is already the main distinguishable feature compared to our method. To deal with long trajectories they rely on a trainable special form of frame skipping where the agent also has to predict how many frames to skip in each situation. This helps to reduce the effective length (step count) of the respective expert trajectories. In contrast to the approach of (Scheller et al., 2020) we rely on a constant frame skip irrespective of the states and actions we are facing. Finally, there are also several common features including:

1. a supervised BC pre-training stage prior to RL fine-tuning,
2. separate networks for policy and value function,
3. independent action heads on top of a sub-sequence LSTM,
4. presenting the inventory state in a certain form to the agent and
5. applying a value-function-burn-in prior to RL fine-tuning.

#### A.4.3 IMPLEMENTATION OF OUR ALGORITHM FOR MINECRAFT

The architecture of the training pipeline incorporates three learning stages:

- sequence alignment and reward redistribution
- learning from demonstrations via behavioral cloning (pre-training) and
- model fine-tuning with reinforcement learning.

Figure A.4 shows a conceptual overview of all components.

**Sequence alignment and reward redistribution.** First, we extract the sequence of states from human demonstrations, transform images into feature vectors using a standard pre-trained network and transform them into a sequence of consecutive state deltas (concatenating image feature vectors and inventory states). We cluster the resulting state deltas and remove clusters with a large number of



Figure A.5: Mapping of clusters to letters.

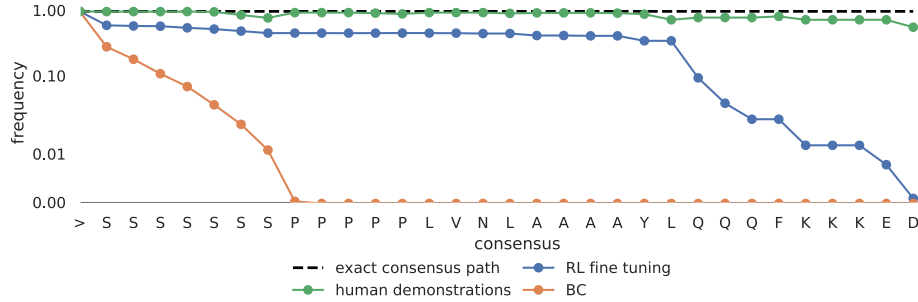


Figure A.6: Comparing the consensus frequencies between behavioral cloning (BC), our model (RL fine tuning) and human demonstrations.

members and merged smaller clusters. This results in 19 events and we map the demonstrations to sequences of events. These events correspond to inventory changes. For each human demonstration we get a sequence of events which we map to letters from the amino acid code, resulting in a sequence of letters. In Fig. A.5 we show all events with their assigned letter encoding that we defined for the Minecraft environment.

We then calculate a scoring matrix according to Eq. (3) in the main document. Then, we perform multiple sequence alignment to align sequences of events of the top  $N$  demonstrations, where shorter demonstrations are ranked higher. This results in a sequence of common events which we denote as the consensus. In order to redistribute the reward, we use the PSSM model and assign the respective reward. Reward redistribution allows the sub-goal definition i.e. positions where the reward redistribution is larger than a threshold or positions where the reward redistribution has a certain value. In our implementation sub-goals are obtained by applying a threshold to the reward redistribution. The main agent is initialized by executing sub-agents according to the alignment.

**Learning from demonstrations via behavioral cloning.** We extract demonstrations for each individual sub-task in the form of sub-sequences taken from all demonstrations. For each sub-task we train an individual sub-agent via behavioral cloning.

**Model fine-tuning with reinforcement learning.** We fine-tune the agent in the environment using PPO (Schulman et al., 2018). During fine-tuning with PPO, an agent receives reward if it manages to reach its sub-goal.

To evaluate the performance of an agent for its current sub-goal, we average the return over multiple roll-outs. This gives us a good estimate of the success rate and if trained models have improved during fine tuning or not. In Fig. A.6, we plot the overall success rate of all models evaluated sequentially from start to end.

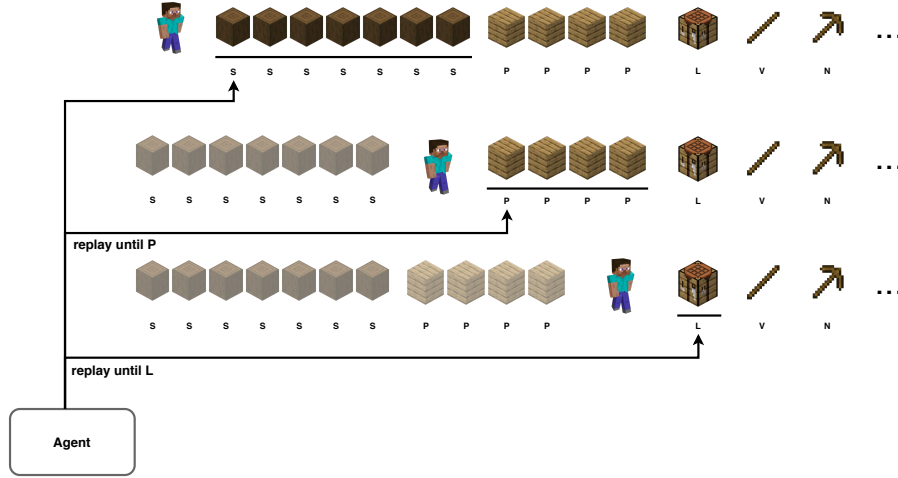


Figure A.7: Trajectory replay given by an exemplary consensus. The agent can execute training or evaluation processes of various sub-tasks by randomly sampling and replaying previously recorded trajectories on environment reset. Each letter defines a task. L (log), P (planks), V (stick), L (crafting table) and N (wooden pickaxe).

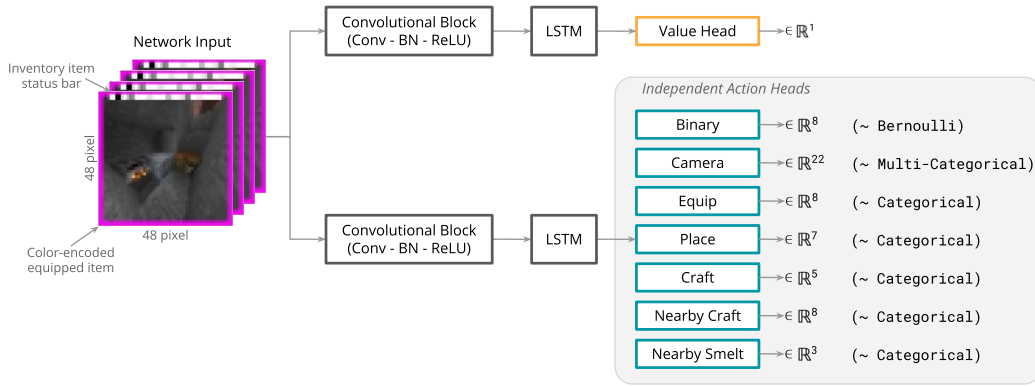


Figure A.8: Conceptual architecture of our MineRL policy and value networks.

In order to shorten the training time of our agent, we use trajectory replay and state resetting, similar to the idea proposed in (Ecoffet et al., 2019), allowing us to train sub-task agents in parallel. This is not necessary for the behavioral cloning stage, since here we can independently train agents according to the extracted sub-goals. However, fine-tuning a sub-task agent with reinforcement learning requires agents for all previous sub-tasks. To fine-tune agents for all sub-tasks, we record successful experiences (states, actions, rewards) for earlier goals and use them to reset the environment where a subsequent agent can start its training. In Fig. A.7, we illustrate a trajectory replay given by an exemplary consensus.

#### A.4.4 POLICY AND VALUE NETWORK ARCHITECTURE

Figure A.8 shows a conceptual overview of the policy and value networks used in our MineRL experiments. The networks are structured as two separate convolutional encoders with an LSTM layer before the respective output layer, without sharing any model parameters.

The input to the model is the sequence of the 32 most recent frames, which are pre-processed in the following way: first, we add the currently equipped item as a color-coded border around each RGB frame. Next, the frames are augmented with an inventory status bar representing all 18 available inventory items (each inventory item is drawn as an item-square consisting of  $3 \times 3$  pixels to the frame). Depending on the item count the respective square is drawn with a linearly interpolated



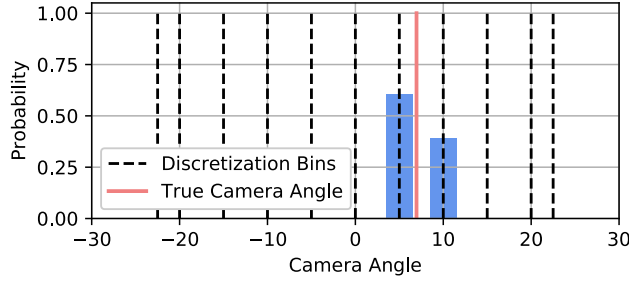


Figure A.9: Discretization and interpolation of camera angles.

gray-scale ranging from white (no item at all) to black (item count  $> 95$ ). The count of 95 is the 75-quantile of the total amount of collected cobblestones and dirt derived from the inventory of all expert trajectories. Intuitively, this count should be related to the current depth (level) where an agent currently is or at least has been throughout the episode. In the last pre-processing step the frames are resized from  $64 \times 64$  to  $48 \times 48$  pixels and divided by 255 resulting in an input value range between zero and one.

The first network stage consists of four batch-normalized convolution layers with ReLU activation functions. The layers are structured as follows: Conv-Layer-1 (16 feature maps, kernel size 4, stride 2, zero padding 1), Conv-Layer-2 (32 feature maps, kernel size 4, stride 2, zero padding 1), Conv-Layer-3 (64 feature maps, kernel size 3, stride 2), and Conv-Layer-4 (32 feature maps, kernel size 3, stride 2). The flattened latent representation ( $\in \mathbb{R}^{32 \times 288}$ ) of the convolution stage is further processed with an LSTM layer with 256 units. Given this recurrent representation we only keep the last time step (e.g. the prediction for the most recent frame).

The value head is a single linear layer without non-linearity predicting the state-value for the most recent state. For action prediction, two types of output heads are used depending on the underlying action distribution. The binary action head represents the actions *attack*, *back*, *forward*, *jump*, *left*, *right*, *sneak* and *sprint* which can be executed concurrently and are therefore modeled based on a *Bernoulli* distribution. Since only one item can be equipped, placed, or crafted at a time these actions are modeled with a *categorical* distribution. The equip head selects from *none*, *air*, *wooden-axe*, *wooden-pickaxe*, *stone-axe*, *stone-pickaxe*, *iron-axe* and *iron-pickaxe*. The place head selects from *none*, *dirt*, *stone*, *cobblestone*, *crafting-table*, *furnace* and *torch*. The craft head selects from *none*, *torch*, *stick*, *planks* and *crafting-table*. Items which have to be crafted nearby are *none*, *wooden-axe*, *wooden-pickaxe*, *stone-axe*, *stone-pickaxe*, *iron-axe*, *iron-pickaxe* and *furnace*. Finally, items which are smelted nearby are *none*, *iron-ingot* and *coal*. For predicting the camera angles (*up/down* as well as *left/right*) we introduce a custom action space outlined in Figure A.9. This space discretizes the possible camera angles into 11 distinct bins for both orientations leading to the 22 output neurons of the camera action head. Each bin holds the probability for sampling the corresponding angle as a camera action, since in most of the cases the true camera angle lies in between two such bins. We share the bin selection probability by linear interpolation with respect to the distance of the neighboring bin centers to the true camera angle. This way we are able to train the model with standard categorical cross-entropy during behavioral cloning and sample actions from this categorical distribution during exploration and agent deployment.

#### A.4.5 IMITATION LEARNING OF SUB-TASK AGENTS

Given the sub-sequences of expert data separated by task and the network architectures described above we perform imitation learning via behavioral cloning (BC) on the expert demonstrations. All sub-task policy networks are trained with a cross-entropy loss on the respective action distributions using stochastic gradient descent with a learning rate of 0.01 and a momentum of 0.9. Mini-batches of size 256 are sampled uniformly from the set of sub-task sequences. As we have the MineRL simulator available during training we are able to include all sub-sequences in the training set and evaluate the performance of the model by deploying it in the environment every 10 training epochs. Once training over 300 epochs is complete we select the model checkpoint based on the total count

---

of collected target items over 12 evaluation trials per checkpoint. Due to presence of only successful sequences, the separate value network is not pre-trained with BC.

#### A.4.6 REINFORCEMENT LEARNING ON SUB-TASK AGENTS

After the pretraining of the Sub-Task agents, we further fine tune the agents using PPO in the MineRL environment. The reward is the redistributed reward given by Align-RUDDER. The value function is initialized in a burn-in stage prior to policy improvement where the agent interacts with the environment for 50k timesteps and only updates the value function. Finally, both policy and the value function are trained jointly for all sub-tasks. All agents are trained between 50k timesteps and 500k timesteps. We evaluate each agent periodically during training and in the end select the best performing agent per sub-task.